THEORETICAL CHEMISTRY INSTITUTE

THE UNIVERSITY OF WISCONSIN

ENTROPY AND CHEMICAL CHANGE. I. CHARACTERIZATION OF PRODUCT (AND REACTANT) ENERGY DISTRIBUTIONS IN REACTIVE MOLECULAR COLLISIONS: INFORMATION AND ENTROPY DEFICIENCY

R. B. Bernstein and R. D. Levine

WIS-TCI-472

7 March 1972

MADISON, WISCONSIN

Entropy and Chemical Change. I. Characterization of Product (and Reactant) Energy Distributions in Reactive Molecular Collisions: Information and Entropy Deficiency*

R. B. Bernstein

Chemistry Department and Theoretical Chemistry Institute
University of Wisconsin, Madison, Wisconsin 53706

and

R. D. Levine†+

Department of Chemistry, The Ohio State University
Columbus, Ohio 43210

ABSTRACT

The present paper considers optimal means of characterizing the distribution of product energy states resulting from reactive collisions of molecules with restricted distributions of initial states, and vice versa, i.e., characterizing the particular reactant state distribution which yields a given set of product states, at a specified total energy E. The $\underset{\sim}{S}$-matrix, or reaction probability matrix $\underset{\sim}{P}(E)$, "global" in nature, contains much more detail than necessary to reproduce the results of any single specific experiment or computer-simulation thereof (via classical mechanical trajectory calculations). Moreover, since reactant and/or product state resolution is always experimentally

- - - - -

* This work received suppott from the National Science Foundation, Grant GP-26014, National Aeronautics and Space Administration Grant NGL 50-002-001 and the Air Force Office of Scientific Research, Grant XXX-0000.

† Alfred P. Sloan Fellow. +Also at Department of Physical Chemistry, The Hebrew University, Jerusalem, Israel.

limited (to a greater or lesser degree), data are necessarily coarse-grained accordingly. Many quantal features are thereby lost and the results are often at a level appropriate for comparison with classical calculations (e.g., in the form of low-resolution contour maps of energy disposal). Such contour plots of the yield function Y or the averaged transition probability ω (the "poor-man's" $\underset{\sim}{P}$-matrix) nevertheless contain the essence of the dynamical results. It is suggested to represent the energy-dependence of global-type results in the form of square-faced bar plots, and of data for specific-type experiments (or computer simulations) as triangular-faced prismatic plots (contour maps vs. E). The essential parameters defining the internal state distribution are isolated, and the information content $I(E)$ of such a distribution (for a micro-canonical ensemble) is put on a quantitative basis. The relationship between the information content, the surprisal, and the entropy of the continuous distribution is established. The concept of an "entropy deficiency" $\Delta S'$, which characterizes the specificity of product state formation, is suggested as a useful measure of the deviance from statistical ("phase-space dominated") behavior. The degradation of information by experimental averaging is considered, leading to bounds on the entropy deficiency.

1. Introduction

Important information on the dynamics of reactive molecular collisions is derived from a knowledge of the distribution of internal energy states of the products or the relative reactivity of reactants in different excited internal states[1-21].

In the present paper, for simplicity we restrict our attention to the simplest case of a three-center, atom-transfer reaction of the type $A + BC \rightarrow AB^{\dagger} + C$, where the dagger denotes internal excitation of the product diatomic. An example is the hydrogen-abstraction reaction:

$$C\ell + HI(v,J) \rightarrow HC\ell(v',J') + I, \qquad (1)$$

one of a number of three-center reactions which have been well-studied via the infrared chemiluminescence technique by Polanyi and his followers[1-5].

Ordinarily the initial internal state (v,J) distribution has been essentially Boltzmann, fixed by the temperature of the reactant molecules BC. The experimental measurements yield the internal state distribution (v',J') of the product molecules $AB^{\dagger}$, often found to be non-Boltzmann in character. In many cases extensive population inversion occurs, thereby providing the basis of chemical laser action[2b].

With the exception of the hydrides, the resolution of individual internal quantum states of the products has not yet been feasible. For most practical purposes, when the density of internal states is high, it is therefore convenient to regard the internal energies as continuous variables, say $E_{V'}$ and $E_{R'}$, representing product vibrational and rotational energies, respectively. Even when individual states have been resolved, it is often useful to "smear out" the discrete distribution to convey a qualitative picture of the overall experimental results. Moreover, with the wide utilization of classical mechanical trajectory calculations and Monte Carlo evaluation of reactive scattering cross sections it behooves us to adapt to classical, continuous probability density functions, histograms and "bins", rather than to attempt to "quantize" artificially the classically calculated results. In sections 2-4 and 9 we will concern ourselves mainly with coarse-grained product (and reactant) energy distributions.

Given the internal energy distribution of product ($AB^{\dagger}$) molecules one can immediately calculate the distribution of relative translational

energy, $E_{T'}$, of the recoiling products[6], making use of the energy conservation relation:

$$E = E_{T'} + E_{V'} + E_{R'} = E_T + E_V + E_R - \Delta E_o \quad . \qquad (2)$$

Here E is the total energy, made up of the initial relative translational energy of the A + BC system, E_T, the vibrational and rotational energies, E_V and E_R, of the reactant molecule BC, and the zero-point to zero-point reaction exoergicity, $-\Delta E_o$. The translational distribution of products can be measured directly, in the course of molecular beam scattering experiments, via the velocity analysis technique[7-9]. The crossed molecular beam method has also yielded more direct information on product state distributions[10]. For a number of reactions it has been possible to carry out rotational state analysis,[11,12] and, more recently, vibrational state analysis has been accomplished[13,14]. The chemical laser technique, as pioneered by Pimentel and co-workers, has provided independent data on relative populations of vibrational states of product molecules,[15,16] which are directly comparable with the ir chemiluminescence results. It is clear that the question of the energy disposal in elementary exoergic reactions is of great importance in the field of modern chemical kinetics.

Alternative information on microscopic chemical reaction dynamics is available from experiments involving reactants in excited internal states. Thus far such studies have been concerned with endoergic reactions or those with an energy barrier to be surmounted. The influence of reactant internal energy $E_{int} \equiv E_V + E_R$, controlled by the temperature of the BC molecule, at constant E_T, has been studied in one such case by Schmeltekopf et al.,[17] and the separate effect upon the reaction cross section of E_V at fixed E_R and E_T has been investigated by Chupka et al.,[18] and by Brooks and co-workers[19]. The possibility of utilizing judicious vibrational excitation of reactants for selective influence of the product molecular configuration has already been considered[20], and selective excitation by lasers is now a rapidly developing field[21] with many practical implications.[22]

The considerable experimental activity in this field has stimulated much theoretical interest[23]. Anlauf et al.[24] pointed out the utility of microscopic reversibility to gain information on the influence of reactant excitation upon the rate of an endoergic reaction, based upon product

internal state distributions for the exoergic reaction. Kinsey[25] showed how such considerations could be most fully exploited when only limited data of various types on the exoergic reaction are available. Marcus[26] further investigated these same questions and showed the relationship to the quasi-equilibrium approximation. The simplistic optical model analysis[23,27] has also been used in this area, interrelating the forward and reverse reaction cross sections. The statistical theory[28-30] has been found to be a useful diagnostic tool, since deviations from its predicted (equilibrium micro-canonical) distribution of product states are a measure of the specific, non-equilibrium nature of the reactive collisions.

The ultimate theoretical description of the dynamics is, of course, a proper dynamical theory. At the present stage there are still formidable obstacles in the path of a full quantal solution of the reactive scattering problem.[31] Thus we turn to classical mechanical, numerical trajectory calculations,[1,23,32-36] which attempt to stimulate experiment assuming a "realistic", adiabatic potential surface and neglect all quantal interference effects. In what follows we shall assume that at least fragmentary, low-resolution data or computer-simulated experimental results are available, and our goal is to extract as much information as possible from the available "data", whether experimental or calculated.

One of the aims of the present paper is to develop optimal means of characterizing the distribution of product states (in a given experiment, at a given total energy), as governed by the reactant state distribution (and vice versa, i.e., the reactant state distribution yielding a given set of product states), in terms of any two of the three energy variables $E_{T'}$, $E_{V'}$, $E_{R'}$. Of course, only two of these are independent quantities (cf. Eq. 2). It will often be convenient to work with fractional quantities f_X, defined as the fraction of the total available energy in the mode X (where X may be T,V,R or the same symbols primed). Throughout the paper attention is restricted to the energy range below the threshold for collision-induced dissociation.

Before proceeding further, it is necessary to distinguish between two classes of data, i.e., "global" and "specific". For a complete statement of the dynamics of the reaction, one requires the transition probabilities from all possible initial states to all possible final states. Such a global representation requires a transition probability matrix, $\underset{\sim}{P}$, whose elements are mod-squared elements of the $\underset{\sim}{S}$-matrix, such as would be provided by a full

quantal solution to the scattering problem. Neither the experimenter nor the classical mechanical computer are as ambitious as the quantum mechanic, however. They are content to describe an incomplete but specific experiment, i.e., a distribution of product states (or product energies) for a given set of initial conditions.

One can further distinguish (within the class of "specific" representations) between a detailed study in which the product distribution is determined for given, specific initial reactant states, and an "inclusive" study which yields the product state distribution averaged over the reactant state distribution. Assuming perfect resolution of internal states, a global description provides the whole $\underset{\sim}{P}$-matrix. A detailed, specific study (later referred to as "clusive") characterizes a column (or a row) of the $\underset{\sim}{P}$-matrix, while an inclusive, specific study provides only an "average" over a row or column.

Sec. 2 considers the presentation of the results of a study of the global dynamics in the form of square-faced "bar" plots; such a plot provides low-resolution probability contour maps (the poor-man's $\underset{\sim}{P}$-matrix). Sec 3 discusses the representation of "specific" results in the form of a triangular-faced "prismatic" plot. The essential parameters defining a given internal state distribution are isolated and discussed in Sec. 4. The "information content" of a product state distribution is considered in Sec. 5. Transition probabilities and the problem of degenerate (or experimentally indistinguishable) states are discussed in Sec. 6 (which is confined to discrete distributions). Sec. 7 is concerned with the information content of the two types of "specific" experiments, as well as the "global" type of results. Sec. 8 summarizes the hierarchy of possible representations that are available for the distribution of products (and influence of the distribution of the reactants). Sec. 9 considers the problem of defining the information content of a continuous distribution. Sec. 10 makes the connection with entropy and suggests the concept of an entropy deficiency characterizing the specificity of the product state distribution. Sec. 11 summarizes the important definitions and results.

2. SQUARE-FACED BAR PLOTS FOR SUMMARIZING RESULTS OF "GLOBAL" EXPERIMENTS

One may "collapse" the transition probability matrix $\underset{\sim}{P}$, at a given E, to a function of two independent variables E_T, $E_{T'}$ (or E_{int}, $E_{int'}$ which are complementary variables). Primes designate products (post-collision variables). The fractions f_T, $f_{T'}$ are convenient reduced variables; thus $f_T = E_T/(E_T)_{max}$ and $f_{T'} = E_{T'}/(E_{T'})_{max}$, where $(E_T)_{max}$, $(E_{T'})_{max}$ are the maximum conservation-allowed values of E_T, $E_{T'}$ respectively (cf. Sec. 1). Thus $1-f_T$ and $1-f_{T'}$ are the reduced internal energy of reactant and product molecules, respectively. Let $\omega(E_T,E_{T'})$ be the average transition probability[25] corresponding to reactants with E_T in the range between E_T and $E_T + dE_T$ forming products with $E_{T'}$ in the range $E_{T'}$, $E_{T'} + dE_{T'}$ (at a given total E). Then

$$\omega(E_T,E_{T'}) = \sum_n' \sum_{n'}' (P_{n',n}) \Big/ \sum_n' \sum_{n'}' (1) \quad . \tag{3}$$

Here n,n' denote the internal states of the reactants and products respectively, $P_{n',n} = |S_{n',n}|^2$ is the $n \to n'$ state-to-state reaction probability and the sums are confined to states n,n' in the specified ranges (corresponding to the E_T,$E_{T'}$ increments). The concept of averaged transition probability (and its symmetry with respect to the interchange of E_T and $E_{T'}$) is further discussed in Secs. 6 and 9. It is of course clear that the concept of a smooth functional dependence of ω on the two variables E_T, $E_{T'}$ implies not only classical mechanics but also a sufficiently high density of internal states so that the dependence on the variables is smooth and the limit implied by (3)(both numerator and denominator are differentials) is well defined. The probability ω can be presented as a contour map in terms of E_T, $E_{T'}$ (as in Fig. 1a) or in terms of f_T, $f_{T'}$ on a unit square (Fig. 1b). Of course we must take cognizance of the relation between the two

$$\omega(E_X)\,dE_X = \omega(f_X)\,df_X \quad . \tag{4}$$

Note that, in general, $\omega(E_T,E_{T'})$ is the same quantity for both the forward and the reverse reaction, and a <u>single</u> contour map is sufficient to characterize the global dynamics at a specific total energy E. Stacking together such squares at successively greater values of E yields a "bar plot", whose cross section is the f_T, $f_{T'}$ plane and long axis and the E scale. The loci of the maximum of (coordinates $f_T^{(m)}$, $f_{T'}^{(m)}$) are plotted <u>vs</u>. E in Fig. 1c.

There are no "global" results available yet, either experimental or computer-generated, even at a single E, although a considerable amount of fragmentary information from different sources is known. For example, data

exist which correspond to vertical or horizontal "slabs" of the bar.

In certain common types of "inclusive" experiments the total reaction cross section into all product internal states is measured as a function of E_T, with reactant internal state distributions essentially Boltzmann, corresponding usually to small f_V, f_R. Thus f_T is maintained at a near-constant value slightly less than unity while E (= $E_T - \Delta E_o$) varies directly with E_T. This measurement of $\sigma(E_T)$ is the most common one in conventional beam experiments, for example in studies involving ionic reagents,[17,18,37] collisional ionization of neutrals,[38-40] and, recently, for neutral reactants yielding neutral products[41]. Such experiments amount to summing (or averaging) over all $f_{T'}$ in a "vertical slab" of a bar-plot such as Fig. 1b.

There are more refined, and thus only partially-inclusive, experiments in which the product translational distribution is measured as a function of E_T[7b] (with the reactant internal state distribution held constant). Here the "vertical slab" has been analyzed in terms of its $f_{T'}$ distribution.

In another type of experiment the reactant internal energy is varied at nearly constant E (or over a small range of E) and the total reaction cross section observed,[17,18,42] but with no translational (or internal) energy analysis of the products. These results correspond to summing over all $f_{T'}$ for a series of successive vertical slabs at given f_T values. An example of such primary data is shown in Fig. 2, constructed from the results of Refs. 17 and 43.

The global results require observations (or computations, at least via classical trajectories) at constant E over an entire square grid of f_T, $f_{T'}$, to establish a contour map at each of several values of E. Such a global bar-plot would have practical implications with regard to optimization of reaction yield. The relative importance of E_T *vs.* E_{int} at given E can be ascertained by inspection of such a contour map. *E.g.*, from Fig. 1a (at E = 10 units), optimum yield of products for the *endoergic* reaction would be obtained if the reactants had a value of E_{int} of 6 units (i.e., $f_T^{(m)} = 0.4$; thus $E_T^{(m)} = 4$ and $E_{int}^{(m)} = 6$ units). Note that the smallest "allowed" value of E is $-\Delta E_o = 5$ units. Information on both forward and reverse reactions is contained in the same contour map. The limitation of a square-faced bar-plot such as that of Fig. 1b is, of course, that distinction is made only between translational and internal energies, whereas we know

that the separate internal modes (rotation and vibration) contribute very differently to the reaction probability. Thus we should consider the "decomposition" of E_{int} into its two "components", E_V and E_R, and their separate effects, as discussed in the next section.

3. TRIANGULAR-FACED PRISMATIC PLOTS FOR SUMMARIZING RESULTS OF "SPECIFIC" EXPERIMENTS

The information content of one type of "specific" experiment, e.g., one in which reactant states are specified, is the coarse-grained distribution of product states represented as functions of any two independent variables of the set $\{E_{T'}, E_{V'}, E_{R'}\}$. We may also consider the inverse of this, i.e., the distribution of reactant states, in terms of $\{E_T, E_V, E_R\}$, which yield a specified distribution of product states corresponding to the same total energy E. If this specified product state distribution is chosen to coincide with the reactant state distribution of the previous experiment, the results of the two experiments are uniquely related via the principle of microscopic reversibility.[24-26] The properly symmetrized measure of reaction probability is either the yield function,[44] Y, or the closely-related averaged transition probability,[25] ω.

The results of a "specific" experiment can be conveniently represented as a contour map in a plane, with contour lines denoting equiprobable final states (or initial states, as the case may be).[24] Of the several possible choices of diagrams (see Appendix 1 for details), the equilaterial triangular one used by Kinsey[25] seems preferable, since it maintains complete symmetry with respect to the three modes T,V,R (or T',V',R'). Such a plot is illustrated schematically in Fig. 3. The coordinate axes are the fractions f_x of the available energy in mode X, and the vertices designated T, V, R represent 100% of the energy in the specified mode, as usual. Of course, any two coordinates of the set $\{f_T, f_V, f_R\}$ suffice to specify the location of a given point. (Note that such a triangular probability contour map is not the same as a triangular map of relative rate constants, as used to display the chemiluminescence results.[1,24,48])

The most significant single characteristic feature of such a continuous state distribution or contour map of reaction probabilities is the location of the maximum probability (and possibly of any subsidiary maxima, not present in the example shown). The coordinates of the maximum are designated $f_T^{(m)}$, $f_V^{(m)}$, $f_R^{(m)}$, any two of which fix the "most probable" location. The next most significant feature of such a state distribution is the "sharpness" of the maximum. This question is discussed in Sec. 4.

Of course the location of the maximum and its intensity (and curvature) will depend upon E, but in general one expects that the energy dependence of the most-probable fraction $f_X^{(m)}$ in mode X will be less severe than that of $E_X^{(m)}$, the most-probable energy[45,46] itself.

In order to display the overall energy dependence of the state distribution one can array a "stack" of such contour maps along a total energy axis, E, perpendicular to the triangular faces, thereby obtaining a prism, as shown in Fig. 4a. Each cut through the prismatic diagram represents the energy partitioning at the specified, constant total E. Fig. 4b summarizes the most significant data, the trajectory of the locus of the maximum yield as a function of E, analogous to that of Fig. 1c.

It should be noted that the entire prismatic plot corresponds to a certain set of initial conditions specified by f_V, f_R or, more commonly, a particular distribution in f_V, f_R. We may thus distinguish between two types of "specific" experiments. The first is an "inclusive" type, where there is a broad distribution of initial reactant conditions (i.e., distribution in f_V, f_R) which give rise to the product distributions in $f_{V'}$, $f_{R'}$, $f_{T'}$ displayed on each triangle. Conversely, for a given specified f_V, f_R one has data only on the total product yield and so the contour map in the triangle summarizes the influence of the initial state distribution in f_V, f_R upon the overall reaction probability. An example of the former is the usual ir chemiluminescence experiment[1] in which Boltzmann distributions of reactants at given temperatures describe the initial conditions and then the experimental results consist of detailed product state distributions, i.e., $\omega(f_{V'}, f_{R'})$ valid for the set $\{\bar{f}_V, \bar{f}_R\}$ at some mean value $\bar{E}$ of the total energy. An example of the inverse is an experiment in which the total reaction cross section (irrespective of product states) is measured as a function of E_V and/or E_R at essentially fixed E, as in Refs. 17-18.

It is clear that the results of such "inclusive", "specific", experiments provide only a limited amount of information on the reverse reaction. This can most easily be seen upon consideration of the square-faced bar-plots of Sec. 2. An inclusive experiment supplies only the (possibly weighted) average (or sum) of entries along a row or column and hence cannot characterize the entire square face.

As an example, consider a simple case of an exoergic reaction (cf. Eq. 1) carried out in a crossed beam experiment, with reactant BC in a Boltzmann internal state distribution (characterized by some temperature T_{int}) and with a given relative translational energy distribution, say Maxwellian (corresponding to some temperature T_{tr}). Suppose that this, inclusive, experiment shows that the product $AB^{\dagger}$ is formed with considerable vibrational excitation. Then all that one may conclude is that, for the reverse reaction, the use of vibrationally excited $AB^{\dagger}$ as a reactant will enhance the rate of formation of BC in an essentially equilibrated Boltzmann internal energy state distribution (characterized by the above-mentioned temperature T_{int})[47]. One cannot rule out the possibility that (for example) an increase in the translational energy ($E_{T'}$) would not be still more advantageous for the production of BC, if no restriction is placed on the degree of excitation of the BC. Classical trajectory calculations would be useful to explore such questions in detail for specific systems[49].

The more detailed information is provided by a specific "clusive" experiment. Here one considers the distribution of products for a sharply defined initial state. The prismatic plots, as in Figs. 3 and 4, represent a complete summary of the energy disposal for the "forward" exoergic reaction, in a specific, clusive experiment (i.e., for a narrow range of f_V, f_R, or, more commonly, at a narrow range of E_V, E_R). A prismatic plot represents an enormous amount of detail, more than we would normally wish to know. Yet, in recording only the energy trajectory of the locus of the maximum in the contours in Fig. 4b, we have sacrificed too much detail. What is needed is to characterize succinctly the contour map in the region of the neighborhood of its maximum. In addition to its coordinates, one requires its "strength" (or magnitude) and its "sharpness" (or curvature). This will be considered in the next section.

4. CHARACTERIZATION OF A PROBABILITY DENSITY ENERGY CONTOUR MAP: "MOST PROBABLE STATES"

From the discussion in the previous section it appears highly desirable to attempt a concise characterization of an internal energy contour map, i.e., to consolidate the overabundant detail of such a map (cf. Fig. 3) by parametrizing its most significant structural features.[50]

Perhaps the simplest characterization is the one originally used by Polanyi and others[3] to summarize the chemiluminescence results. The data are "coarse-grained", by considering the relative rate of formation of product $AB^{\dagger}$ in each excited vibrational state, irrespective of rotational excitation, and then plot the results as $k(f_{V'})$ vs. $f_{V'}$ (where $f_{V'}$ denotes the fraction of the available energy in product vibration).[1,3] Then one calculates the average value of the fraction in vibration, say $\overline{f}_{V'}$. This implies the average fraction of the available energy released into relative translation, by difference, to be $\overline{f}_{T'} = 1 - \overline{f}_{V'}$.

In view of the trend[1,24,25,48] toward the use of the more detailed internal energy contour maps, we should consider the concept of the set of three averages $\{\overline{f}_T, \overline{f}_V, \overline{f}_R\}$. For this we need to locate the "center of gravity" of a triangular probability contour map such as that of Fig. 3. This result will obviously be different than that for a right triangular map of relative rate constants.[1,24,48] For the latter, one could carry out the averaging independently in the two orthogonal directions (f_V, f_R) to obtain $\overline{f}_V$, $\overline{f}_R$. In the absence of experiments, a classical mechanical Monte Carlo computer simulation (for given E_T, E_V, E_R) can readily yield number distributions in $E_{V'}$ and $E_{R'}$ (considered as independent variables) from which the first moments can be found, yielding $\overline{E}_{V'}$ and $\overline{E}_{R'}$, and thus $\overline{f}_{V'}$ and $\overline{f}_{R'}$. (Under certain conditions, the first few moments of a p.d.f. can be directly obtained, with good accuracy, and with relatively few trajectories, without the necessity of computing the entire p.d.f. itself)[51].

However, the thus-obtained average, $\overline{f}_{V'}$, is not the same as the previously mentioned average value of the fraction in vibration, calculated irrespective of the rotational excitation. It is also not true in general that $\overline{f}_{V'} + \overline{f}_{R'}$ equals $1 - \overline{f}_{T'}$. Clearly there are many pitfalls (or at least ambiguities of notation) in discussing such averages, and presumably

there would be similar caveats applied to any "averages" over triangular probability contour maps, such as Fig. 3. These considerations suggest that the characterization of such a map in terms of its "shape" near the maximum is preferable to one in terms of average fractional energy disposals.

Before proceeding further, however, it is worth noting that for all systems thus far studied (either by experiment or computer simulation) the range of relative probabilities ω encompassed by the map is rather large, i.e., ω is usually a strongly varying function of $\{f_X\}$. It is therefore convenient to work with the logarithm rather than the original function itself.

Accordingly we define a new function $I(E_V, E_R)$ by the relation

$$\omega(E_V,E_R) \equiv \exp[-I(E_V,E_R)] \tag{5}$$

where the ω is the probability of Secs. 2 and 3. Similarly I may be defined in terms of any other pair of independent energy variables, such as E_T, E_V, etc.

In view of our preference to represent the results in terms of reduced variables, f_X, e.g., in the triangular contour maps such as Fig. 3, we redefine I accordingly (noting the differential range relationship of Eq. 4), so that

$$I(f_V,f_R) \equiv -\ln\omega(f_V,f_R) \tag{6a}$$

$$I(f_{T'},f_{V'}) \equiv -\ln\omega(f_{T'},f_{V'}) \tag{6b}$$

and so forth, depending upon the choice of independent variables. In what follows, to simplify notation, the two independent variables will be designated x,y.

The locus of the "most probable final state", $x^{(m)}$, $y^{(m)}$ may then be determined by solving

$$[\partial I(x,y)/\partial x]_{x^{(m)}} = [\partial I(x,y)/\partial y]_{y^{(m)}} = 0. \tag{7}$$

The sharpness of the minimum in I(x,y) is governed by the magnitude of the three second derivatives or "force constants", here designated

k_{xx}, k_{xy}, k_{yy}, defined in the obvious manner:

$$k_{xx} \equiv [\partial^2 I(x,y)/\partial x^2]_{x^{(m)},y^{(m)}}$$

$$k_{xy} \equiv [\partial^2 I(x,y)/\partial x \partial y]_{x^{(m)},y^{(m)}} \quad , \text{ etc.} \tag{8}$$

In the neighborhood of the "most-probable state"; $x^{(m)}$, $y^{(m)}$, we can expand I(x,y) and truncate beyond the quadratic terms. This should provide a "poor-man's characterization" of the contour map of the p.d.f. at the specified E. Thus we write

$$I(x,y) \cong I(x^{(m)},y^{(m)}) + \frac{1}{2} k_{xx}[x-x^{(m)}]^2 + k_{xy}[(x-x^{(m)})(y-y^{(m)})] + \frac{1}{2}k_{yy}[y-y^{(m)}]^2. \tag{9}$$

Unfortunately, even the truncated expression (9) requires a knowledge of six parameters (two for the locus of the maximum, one for its strength and three "force constants"), all of which may be expected to be E-dependent. One can simplify the parametrization of the I(x,y) surface by choosing a new pair of coordinates, say u,w, such that

$$I(u,w) = I(0,0) + \frac{1}{2} k_u u^2 + \frac{1}{2} k_w w^2. \tag{10}$$

Such a "normal mode" transformation is readily effected by diagonalizing the quadratic form (9); the details are briefly summarized in Appendix I. Since the transformation involves a rotation it requires the specification of one angle. Thus the three original force constants have effectively been replaced by two new ones plus an angle. The hope is that this angle will be only slightly energy-dependent, and so there may only be four paramters which vary significantly with E, of which two of them (the force constants k_u, k_w) might be expected to be fairly insensitive to E (cf. the implications of the hypothetical Fig. 4a).

There are, of course, intermediate levels of detail, providing more information than just a "poor-man's" specification, yet not as detailed as the whole probability contour map. One may specify a distribution for one independent variable only, either by holding the other variable constant or by integrating over all possible values of

the other variable, as described earlier. The former corresponds to a cut along the prismatic plot, the cut line being the line of constant f_x. In particular, such a cut can be made for $f_x = f_x^{(m)}$, showing the distribution with respect to the other two variables, or along an edge ($f_x = 0$). The latter is more common (cf. Fig. 2). Note that the most probable value of f_y can be determined correctly from a cut at $f_x^{(m)}$ but not necessarily from an edge cut (or a cut at any other value of f_x). Only if the two variables are truly independent (i.e., if $k_{xy} = 0$) or "uncoupled", are two cuts sufficient to determine the distribution.

In the next section we shall consider the implications of the shape of these p.d.f.'s with respect to information content.

5. INFORMATION CONTENT OF A PRODUCT STATE DISTRIBUTION

One notes upon inspection of a smooth distribution of product energies (such as the contour map of Fig. 3) or a cut through such a distribution (cf. Fig. 2), that there is more "information content" in a narrow distribution (where most of the reaction probability is concentrated in the vicinity of the "most probable state") than in a broad distribution. Alternatively stated, there is less "missing information"[52-55] in a narrow distribution. If we know that the distribution is narrow we predict with more confidence that in a future "experiment" most of the products will be "found" near the maximum of the distribution. The broader the distribution, the less our ability to make useful forecasts, as we are missing too much information. Clearly, a uniform distribution represents the maximal state of ignorance to predict the outcome of a given "experiment". A narrow distribution (the analog of a loaded die) implies that the situation is biased, favoring our ability to forecast the result of a future "experiment" with more confidence.

The arguments above apply, of course, to any p.d.f.; Shannon[52] and others[53,54] have formalized these arguments by the itroduction of a quantitative measure of the uncertainty associated with any distribution. The more the information content of the distribution, the lesser our uncertainty about the outcome. In an "experiment" with a definite outcome, the uncertainty is zero. In an "experiment" with a set of equally probable results, the uncertainty is maximal.

The concept of the information content of a set of discrete results of experiments has been fully dealt with in the literature,[52-55] based on probabilistic and statistical considerations. It is noted that the number of ways in which N experiments can result in n different outcomes, with m_1 experiments yielding outcome number 1, m_i experiments yielding the i'th outcome, etc., is given by[56]

$$W = N! / \prod_{i=1}^{n} m_i! \qquad (11)$$

where $\sum_{i=1}^{n} m_i = N$.

Let $P_i = m_i/N$ be the inherent probability of the i'th outcome. Then

$$W = N! / \prod_{i=1}^{n} (NP_i)! \qquad (12)$$

If all outcomes are equally probable, $P_i = P_j = \ldots = \frac{1}{n}$, then

$$W = N!/[(N/n)!]^n \tag{13}$$

so that for large N, n we obtain (using Stirling's approximation)

$$\log W = N \log n. \tag{14a}$$

On the other hand, if only a single outcome is possible, *i.e.*, say $P_j = 1$ and all $P_k = 0$ $(k \neq j)$, then $W = 1$ and

$$\log W = 0. \tag{14b}$$

The quantitative measure of information is usually taken to be

$$I = \log W \tag{15}$$

such that the uncertainty associated with a pair of independent "experiments" is the sum of the independent uncertainties.

Eq. 12 can be rewritten for large N, n and combined with Eq. 15 to yield:

$$I = -N \sum_{i=1}^{n} P_i \log P_i \quad . \tag{16}$$

This is an extensive quantity. To obtain the result "per experiment", this is usually divided by N and written

$$I = -\Sigma P_i \lg P_i \tag{17}$$

It is usual to consider the logarithm to be to the base 2, here designated lg.

Note that I is a non-negative quantity. It ranges from zero (*cf.* Eq.(14b)), when the outcome is certain, to its maximum value (when $P_i = \frac{1}{n}$) of lg n (*cf.* Eq.(14a)) and so is a measure of the "missing" information content.

In the subsequent sections we shall develop the concept of the information content measure which is appropriate to the different representations of product state distributions (both global and specific). Towards this eventual goal we consider in the next section the construct of the averaged transition probability.

6. TRANSITION PROBABILITIES: DISCRETE DISTRIBUTIONS

Let n and n' be the sets of quantum numbers required to fully specify the quantal states for the reactants and products respectively. In general, the experimental arrangement is such that one is unable, in principle, to fully resolve the internal states[57]. The experimentally indistinguishable states are collected together in the group γ. Suppose there are $g_{\gamma'}$ final states in the group γ'. The averaged transition probability from an initial state in the group γ to a final state in the group γ' is then given by[25]

$$\omega(\gamma\to\gamma') = (g_\gamma g_{\gamma'})^{-1} \sum_{n'\epsilon\gamma'} \sum_{n\epsilon\gamma} P_{n',n} \quad . \tag{18}$$

Here $P_{n',n}$ is the detailed, quantal, state-to-state transition probability; the notation means a summation over those states n included in the group γ. Subject to the reservations discussed in Appendix II, microscopic reversibility[25,58,59] holds, i.e.

$$\omega(\gamma\to\gamma') = \omega(\gamma'\to\gamma) \equiv \omega(\gamma,\gamma') \tag{19}$$

The limitations of Eq. (19) should be clearly understood. What is implied is that only one $\omega(\gamma,\gamma')$ is necessary to specify both the forward and the reverse probabilities. This does not imply that a matrix of elements $\omega(\gamma,\gamma')$ is symmetric. (In fact such a matrix will not, in general, be square). Nor that if $\omega(\gamma,\gamma')$ is small then the rate of the reverse reaction from state γ' to all possible states is necessarily small.

In any particular experiment (or in any particular plot) the specification of the initial state may use a coarse-grained scheme that is less detailed than the groups of indistinguishable states γ, (say, $\Gamma \equiv$ all states having internal energy in a given interval). Let Γ be the set of possible initial groups of states. If P_γ is the probability of finding the system in the initial group γ, $(\gamma\epsilon\Gamma)$, the transition probability into the final group γ' is thus[59]

$$P_{\gamma'} = \sum_{\gamma\epsilon\Gamma} P_\gamma \omega(\gamma,\gamma') g_{\gamma'} \equiv \bar{\omega}(\gamma') g_{\gamma'} \tag{20a}$$

where

$$\bar{\omega}(\gamma') \equiv \omega(\Gamma,\gamma') \tag{20b}$$

(Note that $P_{\gamma'}$ is just the fractional or relative rate $(k_{\gamma'}/\Sigma_{\gamma'} k_{\gamma'})$ of reaction into the product group γ'). When the initial state is definitely in a particular group γ, (i.e. $P_\gamma = 1$),

$$P_{\gamma'} = \omega(\gamma,\gamma')g_{\gamma'} = g_\gamma^{-1} \sum_{n'\epsilon\gamma'} \sum_{n\epsilon\gamma} P_{n',n} \tag{21}$$

corresponding to the usual procedure of averaging over initial states and summing over final states.

One can consider either of two (time-reversal invariant) probabilities, either $\omega(\gamma,\gamma')$, the averaged probability (which, as is clear from Eq. (18) is bounded by 1), or the yield[59]

$$Y(\gamma,\gamma') = g_\gamma g_{\gamma'}\omega(\gamma,\gamma') \quad . \tag{22}$$

When the initial state is prepared without any attempt to resolve the states within the group Γ then P_γ is simply proportional to g_γ and hence

$$P_{\gamma'} = \sum_\gamma{}'(P_\gamma/g_\gamma)\, Y(\gamma,\gamma') \tag{23}$$

(Note that $P_\gamma \propto g_\gamma$ is the equilibrium condition for the microcanonical ensemble, i.e. for an ensemble where the total energy is in the range E to E + dE, all quantum states are equally likely.[61,62])

The formal theory supporting these results is summarized in Appendix II.

As an example of such averaging procedures, consider global data. We restrict attention in this section to the discrete case. A particular entry in a poor-man's P-matrix is

$$\omega(\Gamma,\Gamma') = \sum_\gamma{}' \sum_{\gamma'}{}' g_\gamma g_{\gamma'}\omega(\gamma,\gamma') / \sum_\gamma{}' g_\gamma \sum_{\gamma'}{}' g_{\gamma'} \tag{24}$$

Using Eqs. (21-23), this expression becomes:

$$\omega(\Gamma,\Gamma') = \sum_\gamma{}' \sum_{\gamma'}{}' Y(\gamma,\gamma') / \sum_\gamma{}' g_\gamma \sum_{\gamma'}{}' g_{\gamma'} = \sum_{n\epsilon\gamma} \sum_{n'\epsilon\gamma'} P_{n',n} / \sum_n{}' 1 \sum_{n'}{}' 1 \tag{25}$$

Here the primed summations are over γ and γ' (or n and n') in the range corresponding to the entry in question. (The analogous results for the case of continuous internal energies are developed explicitly in Sec.9).

Next we consider a specific-type experiment, where the initial conditions are identical to those specified previously in ω but the final distribution of products is known. The triangle plot (cf. Fig. 3) can then be expressed in terms of

$$\bar{\omega}(\gamma') = \Sigma'_{\gamma} P_{\gamma}\omega(\gamma,\gamma') \qquad ,\gamma\epsilon\Gamma \ . \tag{26}$$

Thus

$$\omega(\Gamma,\Gamma') = \Sigma'_{\gamma'} g_{\gamma'}\bar{\omega}(\gamma') \Big/ \Sigma'_{\gamma'} g_{\gamma'} \quad , \ \gamma'\epsilon\Gamma' \ . \tag{27}$$

All the information down a given vertical slab of a bar plot (which corresponds to specified initial conditions) can be obtained from a triangle plot for the appropriate specific-type experiment. The necessary modifications for continuous distributions are given in Sec. 9.

7. INFORMATION CONTENT: SPECIFIC EXPERIMENTS

In this section we consider the information content of the product state distribution for the case when a partial resolution of quantum states is possible. (Continuous distributions are deferred until Sec. 9).

The averaged (over the group γ') probability of finding the products in the state n' is (cf. Eq.(20))

$$P_{n'} = P_{\gamma'}/g_{\gamma'} \quad . \tag{28}$$

For the case of an "inclusive" specific experiment this becomes (cf. (20))

$$P_{n'} = \Sigma'_{\gamma} P_{\gamma} \omega(\gamma,\gamma') = \bar{\omega}(\gamma') \tag{29}$$

and for a non-inclusive ("clusive) specific experiment

$$P_{n'} = \omega(\gamma,\gamma') \quad . \tag{30}$$

In both cases

$$\sum_{\gamma'} P_{\gamma'} = \sum_{n'} P_{n'} = 1. \tag{31}$$

It should be clearly stated that (28) assigns equal probability to all the states within the group γ'. (Recall that final states within the group γ' are, in principle, indistinguishable, under the experimental conditions used[57].).

The information associated with this product distribution is, from Eq. (17)

$$\begin{aligned} I_P &= -\sum_{n'} P_{n'} \lg P_{n'} \\ &= -\sum_{\gamma'} \sum_{n' \in \gamma'} (P_{\gamma'}/g_{\gamma'}) \lg (P_{\gamma'}/g_{\gamma'}) \\ &= -\sum_{\gamma'} P_{\gamma'} \lg (P_{\gamma'}/g_{\gamma'}) \\ &\equiv \sum_{\gamma'} P_{\gamma'} I_P(\gamma') \end{aligned} \tag{32}$$

where in the second line the inner summation is over $g_{\gamma'}$, identical terms. The fourth line serves to define a quantity $I_p(\gamma')$, to be referred to shortly.

Given the experimental product state distribution and thus the $P_{\gamma'}$, one can obtain I_p via Eq. (32) as

$$I_p = -\langle \lg(P_{\gamma'}/g_{\gamma'}) \rangle \tag{33}$$

where the average is over the final product distribution. I_p is clearly bounded:

$$0 \leq I_p \leq \lg(\Sigma_{\gamma'} g_{\gamma'}) \quad . \tag{34}$$

The lower bound corresponds to all the products being in one particular group while the upper bound is the microcanonical equilibrium distribution, i.e. when $P_{\gamma'} \propto g_{\gamma'}$ (so that the probability of the products being in the group is proportional to the number of states in the group (cf. Sec. 6)). These results are essentially those already given in Sec. 5, Eqs. (14a,b) with Eq. (17) for I.

I_p is a measure of the information content of the whole distribution. We can also define an information measure of a particular outcome, say γ'. This quantity has been termed[62] the "surprisal". It has been anticipated in Eq. (32) and is defined by

$$I_p(\gamma') = -\lg(P_{\gamma'}/g_{\gamma'}) = -\lg\bar{\omega}(\gamma') \quad . \tag{35}$$

Thus I_p is the average value of the surprisal:

$$I_p = \Sigma_{\gamma'} P_{\gamma'} I_p(\gamma') = -\Sigma_{\gamma'} P_{\gamma'} \lg[\bar{\omega}(\gamma')] = \langle I_p(\gamma') \rangle \quad . \tag{36}$$

Eq. (36) and its implications noted below are the main results of this section. The information content of a distribution is the average of the information contents of the particular groups, each group corresponding to a possible outcome of the reaction. (By definition, we are unable to distinguish between the members of any specific group).

It is of interest to compare the surprisal for the two types of specific experiments, the "clusive" and the "inclusive". For the former the surprisal for a particular outcome is

$$I_p(\gamma,\gamma') = -\lg[\omega(\gamma,\gamma')] , \tag{37}$$

Here $I_p(\gamma,\gamma')$ is the clusive information measure of the outcome γ' for the initial group of states γ. In an inclusive experiment one necessarily first averages over the entire distribution of unresolved initial groups of states

$$\bar{\omega}(\gamma') = \sum_{\gamma}{}' P_\gamma \omega(\gamma,\gamma') \tag{38}$$

and then obtains the information measure (cf. Eq. (20))

$$I_p(\gamma') = -\lg[\bar{\omega}(\gamma')] = -\lg[\sum_{\gamma}{}' P_\gamma \omega(\gamma,\gamma')] \tag{39}$$

It follows from the inequality for convex functions[54,63] that

$$I_p(\gamma') \geq \sum_{\gamma}{}' P_\gamma \, I_p(\gamma,\gamma') . \tag{40}$$

If we now average these surprisals over all final states to obtain the information associated with the overall product distribution, following the procedure of Eqs. (32) and (36), we see that the value of I_p for the inclusive case (obtained by averaging the l.h.s. of Eq. (40) over all γ') is greater than the I_p for the clusive case (from the r.h.s. of Eq. (40)). The latter is closer to being the "true" or intrinsic information associated with the product distribution for the specific experiment.

Instead of considering the product information measure I_p, one can consider the information defect with respect to a microcanonical equilibrium situation (e.g., Eq. (33) vs. the upper bound of Eq. (34)).

We propose to measure the information defect by the average deviation of $I_p(\gamma')$ from its microcanonical equilibrium value

$$\Delta I_p \equiv \langle [I_p(\gamma')]_{eq} - I_p(\gamma') \rangle \tag{41}$$

We note that for a microcanonical equilibrium situation at a given total energy E in the small interval between E and E + dE, all quantum states are equally probable (a microcanonical ensemble), hence

$$(P_{\gamma'})_{eq} = g_{\gamma'} / \sum_{\gamma'} g_{\gamma'} \tag{42}$$

and

$$[I_p(\gamma')]_{eq} = -\lg(\Sigma_{\gamma'} g_{\gamma'}) = -\lg[(P_{\gamma'})_{eq}/g_{\gamma'}] \tag{43}$$

Thus, the information defect is

$$\Delta I_p = \Sigma_{\gamma'} P_{\gamma'} \lg [P_{\gamma'}/(P_{\gamma'})_{eq}] . \tag{44}$$

It is expected that $\Delta I_p \geq 0$, with equality holding only for equilibrium. This follows from Shannon's Lemma: If $\Sigma_{\gamma'} P_{\gamma'} = 1$ and $\Sigma_{\gamma'} (P_{\gamma'})_{eq} = 1$, then, since $\lg x \geq 1 - x^{-1}$, with equality if $x = 1$, then

$$\Delta I_p \geq \Sigma_{\gamma'} P_{\gamma'} [1-(P_{\gamma'})_{eq}/P_{\gamma'}] = \Sigma_{\gamma'} P_{\gamma'} - \Sigma_{\gamma'} (P_{\gamma'})_{eq} = 0. \tag{45}$$

Thus, for any non-equilibrium distribution there is a net positive information defect, relative to the (microcanonical) equilibrium distribution. (A small ΔI_p implies a more uniform distribution, a large ΔI_p a more sharply peaked distribution.)

Based on the results following Eq. (40), it is seen that the information defect for an "imperfect", inclusive type experiment will be less than the intrinsic value of the information defect as obtained from an ideal clusive type specific experiment i.e.,

$$(\Delta I_p)_{clusive} \geq (\Delta I_p)_{inclusive} \geq 0 . \tag{46}$$

Of course, $(\Delta I_p)_{clusive}$ is the more correct characterization of the specific experiment. It is bounded from above by the information defect for the (microcanonical) equilibrium distribution.

The equivalence between I_p and the thermodynamic concept of entropy was shown by Jaynes[53] and Khinchin,[54] based essentially on Shannon's[52] work. This will be employed and extended to deal with the present application in Sec. 10.

8. GLOBAL AND SPECIFIC REPRESENTATIONS.

We have introduced a hierarchy of representations, depending on the resolution obtained, which can be summarized as follows.

(a) Global clusive. This is the most detailed characterization of the reaction possible (in principle) at a given total energy and specified experimental conditions. It corresponds to a complete specification of $\omega(\gamma,\gamma')$ for all possible groups of inital and final states. $\omega(\gamma,\gamma')$is the "rich experimentalist's" $\underset{\sim}{P}$-matrix. In contrast, the rich quantum theorist considers $P_{n',n}$ as the elements of the $\underset{\sim}{P}$-matrix. However, under given conditions the experimentalist can only determine the average of $P_{n',n}$ over $n\varepsilon\gamma$ and $n'\varepsilon\gamma'$ (cf. (18)).

(b) Specific clusive. The most detailed summary of the specific ideal experiment, showing the distribution of products $\omega(\gamma,\gamma')$ for some initial group of states γ. A specific clusive experiment is equivalent to a column of the global clusive representation.

When one goes over to a continuous distribution of products (i.e., the classical limit) the specific clusive representation is the result of a classical trajectory calculation. Figures 3 and 4 are specific clusive representations.

The current state of the experimental art has not yet reached the stage where both the initial and final states can be fully specified. The following three representations take cognizance of this fact, by averaging over either the detailed distribution of the reactants or of the products or both. We can thus consider the following.

(c) Specific inclusive. The detailed distribution $\omega(\Gamma,\gamma')$ of products from some initial ensemble Γ. This is the distribution most commonly obtained from chemiluminescence experiments[1-5] and, as discussed before (cf. (46)), provides an information deficiency that is nearer to the equilibrium value than that obtained from clusive experiments. Very recent results[64] have now provided an insight into the dependence of $\omega(\Gamma,\gamma')$ on the initial ensemble Γ. Alternatively, one can also consider $\omega(\gamma,\Gamma')$, the influence of the reactants' state selection on the probability of formation of products.

(d) Global inclusive. A poor man's $\underset{\sim}{P}$-matrix, in the form of $\omega(\Gamma,\Gamma')$, say $\omega(f_T, f_{T'})$, as shown in Figs. 1 and 5. An entry in the global inclusive representation can be obtained by an averaging of $\omega(\Gamma,\gamma')$ (or $\omega(\gamma,\Gamma')$) over $\gamma',\gamma'\epsilon\Gamma'$ (or over $\gamma\epsilon\Gamma$), as shown in Fig. 5. Along the same lines as the proof of (40) one can prove that the surprisal associated with $\omega(\Gamma,\Gamma')$ (i.e., $-\lg\ \omega(\Gamma,\Gamma')$) is larger than the average of the surprisals of $\omega(\Gamma,\gamma')$. Thus, an equivalent statement to (46) obtains. A poor man's $\underset{\sim}{P}$-matrix is nearer to an "equilibrium" distribution than a rich man's $\underset{\sim}{P}$-matrix. Any averaging necessarily reduces the information deficiency and brings the resulting distribution nearer to the equilibrium (or statistical) limit. To a certain extent, the success of the statistical theory[28,29] depends on this degradation of information by averaging.

(e) Inclusive. The direct experimental determination of a column of the global inclusive $\underset{\sim}{P}$-matrix. Here one is concerned with transitions between some averaged set of reactants (Γ) to an averaged set of products (Γ'), reporting the dependence of $\omega(\Gamma,\Gamma')$ either on Γ' (the averaged distribution of products) or on Γ (the averaged role of reactant excitation). Molecular beam experiments with velocity analysis[7-9] provide the $f_{T'}$ dependence of $\omega(\Gamma,f_{T'})$. The pioneering studies of the influence of reactant internal energy were also of this type.

9. INFORMATION CONTENT OF A CONTINUOUS DISTRIBUTION

As discussed in the earlier sections, individual quantum states are often not resolved and one observes continuous rather than discrete product state distributions. Problems involving continuous distributions are reputed to be more difficult[53,55] because the concept of "equal probability" is less clear cut. In the present application, we have dealt with this problem already even for the discrete case. (Recall that the assumption expressed by Eq. (28) is that we assign equal intrinsic probabilities to each state in a group which is, in principle, unresolved experimentally.) Extension to "valid" continuous distributions requires nothing more, beside the conversion of summations over quantum numbers to integrations over energies. Of course, proper care is required to identify equi-probable quantum states; thus appropriate density of states factors are needed.

Our goal is to obtain an explicit expression for the average value of the suprisal, I_p, for the case of a continuous product (or reactant) state distribution. We shall consider E_f as the (continuous) energy corresponding to the formerly discrete variable, say f, which is now (in the "classical case") continuous. Typically this would be the translational energy E_T, (cf. Sec. 2). The group f is the group of states with energies in the interval E_f to $E_f + dE_f$ and $g_f \equiv g_f(E_f)$ is the density of states, so that $g(E_f)\, dE_f$ is the number of states in that energy interval. $P_f \equiv P(E_f)$ is also now a continuous p.d.f., with $P(E_f)\, dE_f$ being the (averaged) probability that the product energy lies in the interval E_f to $E_f + dE_f$. (Similar considerations apply to reactant state distributions.)

The surprisal $I_p(f) \equiv I_p(E_f)$ is also now a continuous function of E_f, with the above interval having the information measure $I_p(E_f)\, dE_f$. By analogy with Eq. (35), we have

$$\begin{aligned} I_p(E_f) &= -\lg[P(E_f)/g(E_f)] \\ &= -\lg[\omega(E_f)] \quad . \end{aligned} \tag{47}$$

Here $\omega(E_f)$ is the averaged transition probability to the group f, where the discrete averaging of Sec. 6 (cf. Eqs. (18) and (20)) is now an average over a small energy interval. The transition probability to the group f is

given by

$$P(E_f)dE_f = \omega(E_f)g(E_f)dE_f \tag{48}$$

(Of course, in practice, this is how one obtains $\omega(E_f)$ from the observations.) Appropriate density-of-states factors (for diatomics in the rigid rotor-harmonic oscillator approximation) suitable for either bar or prism plots, have been provided by Kinsey.[25]

The information content of the distribution is, as in Sec. 7, the average of the surprisal (cf. (32))

$$\begin{aligned} I_p &= \langle I_p(E_f)\rangle = \int df\,\omega(E_f)I_p(E_f) \\ &= \int dE_f\ \omega(E_f)g(E_f)I_p(E_f) \\ &= -\int dE_f P(E_f)\lg[\omega(E_f)]. \end{aligned} \tag{49}$$

In the case of more than one energy variable, e.g., $E_{V'}$, $E_{R'}$ as well as $E_{T'}$, extension of the above should be readily accomplished, taking advantage of the approach of Sec. 4.

In practice the continuous integration in Eq. (49) would be carried out as a summation over energy "bins":

$$I_p = -\sum_{\Delta E_{\gamma'}} P(E_{\gamma'})[\lg\omega(E_{\gamma'})]\Delta E_{\gamma'} \tag{50}$$

(The results should become, asymptotically at least, independent of bin size).

Global results imply a knowledge of the dependence of the reaction probability upon both initial and final energy variables. In the simple case of a bar plot (cf. Sec. 2) one can use either the averaged transition probability $\omega(E_T,E_{T'})$ or the yield $Y(E_T,E_{T'})$. From Eq. (23)

$$P(E_{T'}) = \int dE_T f(E_T)Y(E_T,E_{T'}) \quad , \tag{51}$$

where $g(E_T)f(E_T)dE_T$ is the fraction of initial states with E_T in the range E_T to $E_T + dE_T$. Similarly from Eq. (20)

$$\overline{\omega}(E_{T'}) = \int dE_T g(E_T)f(E_T)\omega(E_T,E_{T'}) \tag{52}$$

Corresponding results hold for the integration over $E_{T'}$.

10. ENTROPY DEFICIENCY OF A PRODUCT STATE DISTRIBUTION

There is a well-established equivalence between information content and the thermodynamic concept of entropy.[52-55,62] In the case of equilibrium distributions the situation is clear cut, but in the present non-equilibrium context it must be admitted that our recipe for assigning probabilities by the equilibrium rule "all quantum states of the same energy are equally probable" is less secure. Nevertheless this is the simplest means of extending the more familiar equivalence to the problem of the characterization of a non-equilibrium product state distribution.[65]

Assuming the validity of the equivalence, we next establish the practical connection between I_p and S in terms of numerical magnitudes and units. From Eq. (17), if I, the "missing information content", is based on the logarithm to the base 2, i.e., $I = \lg W$, then to obtain the usual result for the entropy, $S \cong k \log W$ from Eq. (15) one must write

$$S = (k \log_e 2)\, I_p \tag{53}$$

A measure of the specificity of the reaction is the entropy deficiency in the product state distribution, which can be expressed

$$\Delta S' = (k \log_e 2)\, \Delta I_p \tag{54}$$

with ΔI_p given by Eq. (44). In practical terms, (i.e., for one mole of reaction), the entropy deficiency is thus $\Delta S'(\text{e.u.}) = 1.38 \Delta I_p$. We recall that the units of information[66] are bits, with 1 bit = $\ell g 2$. Since the size of the entropy deficiency $\Delta S'$ is perforce limited (i.e., the bound being commensurate with the magnitude of standard entropy change of reaction ΔS^o) there appears to be an intrinsic upper bound on ΔI_p (bits).

The entropy deficiency would be zero if the product state distribution were that predicted by a phase-space or statistical (density-of-states) theory. For all actual situations $\Delta S'$ is intrinsically positive. In principle, the product state distribution of a clusive specific experiment would be suitable for analysis to ascertain the entropy deficiency $\Delta S'$ of the reaction (although, due to imperfect reactant-state selection and product resolution, it would yield only a lower-limit estimate of $\Delta S'$).

One can recognize a hierarchy of experiments leading to a range of $\Delta S'$ values. In the absence of data, forced to use a statistical theory, we start with $\Delta S' = 0$. As we continuously sharpen the experiments the computed $\Delta S'$ will be larger;[67] finally the limit of well-defined reactant and product states (from a global clusive

representation) would yield the proper intrinsic value of the entropy deficiency for the reaction at the total energy E. Presumably one would then be in a position to consider the overall dependence on E.

Clearly the concept of an entropy deficiency $\Delta S'$ should also be a useful one in characterizing the poor-man's P-matrix.[68] Whether it can be illuminating physically is considered in the second paper in this series. Its relationship to the heuristically valuable concept of an entropy of activation for a canonical system at a temperature T remains to be established.

11. SUMMARIZING REMARKS

This paper has attempted to characterize the product (and reactant) energy distributions obtained in reactive scattering experiments or computer simulations. Suitable forms of plotting results of global or specific-type experiments have been suggested in Secs. 2 and 3 (see Figs. 1, 3, 4). Means of parametrization of specific type results in terms of an expansion around the most-probable states were developed in Sec. 4, with the most compact form being that of Eq. (10).

The question of the information content of a discrete product state distribution was discussed in Secs. 5 - 7 with the important results being those of Eq. (17) for I, Eq. (32) for I_p and Eq. (44) for ΔI_p (the information defect). Sec. 8 summarizes the types of representations used and their interrelations and stresses the concept of the degradation of information by averaging. The information defect, ΔI_p, is shown to decrease with any additional averaging. The intrinsic ΔI_p can only be obtained from clusive experiments. Any less detailed results yield only a lower bound. In Sec. 9 the generalization was made to continuous distributions, with the results for I_p given in Eqs. (49) - (50).

Finally, the concept of entropy deficiency $\Delta S'$ was proposed in Sec. 10 and quantified in Eq. (54).

Obviously there are many theoretical as well as practical ramifications of the present, rather preliminary, investigation. These are currently being pursued.

Acknowledgment

The authors appreciate a number of discussions with their colleagues on many of the topics of this paper. The phrase "entropy and chemical change" arose in a conversation of one of us (R.D.L.) with Professor G.L. Hofacker. We thank Professor P. R. Certain for valuable comments on the manuscript.

APPENDIX I

There are at least three ways in which one can plot a function $I(E_T, E_V, E_R)$ whose variables satisfy a conservation relation, i.e., Eq. (2). (a) An equilateral triangular plot, as discussed in Sec. 3. (b) A cartesian axis plot, as used in Refs. 24, 48, etc. and (c) a triangular plot where the skewing angle is defined so as to diagonalize the function I about the minimum.

The advantage of choices (b) and (c) is the ease of diagonalizing the function. For the cartesian case, one requires a unitary matrix $\underset{\sim}{U}$, say

$$\underset{\sim}{U} = \begin{pmatrix} \cos\theta & \sin\theta \\ -\sin\theta & \cos\theta \end{pmatrix} \tag{A.1}$$

Here θ is determined such that

$$\underset{\sim}{U} \begin{pmatrix} k_{xx} & k_{xy} \\ k_{xy} & k_{yy} \end{pmatrix} \underset{\sim}{U}^{\dagger} = \begin{pmatrix} k_c & 0 \\ 0 & k_s \end{pmatrix} . \tag{A.2}$$

In this case, the maximum is determined by its two coordinates, by the angle θ and the two diagonal derivatives k_c and k_s. Case (a) is analogous to case (b) but requires a pretransformation from the skewed coordinates to cartesian coordinates.

Case (c) is analogous to the method of plotting the potential energy surface for collinear collisions, with the exception that here one chooses the axis not to diagonalize the kinetic energy but what corresponds to the potential energy. In fact, we have loosely referred to the second derivatives of I as the "force constants". This is not simply because of the mathematical analogy but because of "thermodynamic" reasons (to be discussed elsewhere).

Choosing E_V and E_R as the independent variables we scale the E_R axis by c (i.e., to be plotted is E_R/c) and tilt it by the angle θ from the (vertical) Y axis. Thus

$$\begin{aligned} E_R &= c\,Y\sec\theta \\ E_V &= X - Y\tan\theta \end{aligned} \tag{A.3}$$

where E_V is parallel to the X axis. The angle θ is selected to eliminate any cross derivative, i.e.,

$$\left(\frac{\sin\theta}{c}\right) = k_{xy}/k_{yy} \tag{A.4}$$

and the scale c is defined so that $k_Y = k_X$ or

$$c^2 = k_{xx}/k_{yy} \tag{A.5}$$

$$\sin^2\theta = k_{xy}/k_{yy} \quad . \tag{A.6}$$

With these choices,

$$I(X,Y) = I(X^{(m)}, Y^{(m)}) + \frac{1}{2}\rho^2 k^2 \tag{A.7}$$

where

$$\rho^2 = (X - X^{(m)})^2 + (Y - Y^{(m)})^2 \tag{A.8}$$

and $k^2 = k_{xx}$. Superscript (m) denotes the most probable value. In this way the maximum has five parameters ($E_V^{(m)}$, $E_R^{(m)}$, c, θ and k) but only one second derivative.

APPENDIX II

We are concerned with transitions between two sets of states $\Gamma \equiv \{\gamma\}$ and $\Gamma' \equiv \{\gamma'\}$. Let $\rho(\Gamma)$ and $\rho(\Gamma')$ be the appropriate density matrices for the two sets. One can then define the rate constants for the forward and reverse reaction[59,60]

$$k(\Gamma \to \Gamma') = Tr\{\rho(\Gamma) S \rho(\Gamma') S^{\dagger}\} / h\, Tr\{\rho(\Gamma)\} \tag{B.1}$$

and

$$k(\Gamma' \to \Gamma) = Tr\{\rho(\Gamma') S \rho(\Gamma) S^{\dagger}\} / h\, Tr\{\rho(\Gamma')\}. \tag{B.2}$$

In both cases we average over the initial ensemble and sum over the final ensemble. When the states in the group γ cannot be resolved under the given experimental conditions they are taken to be equiprobable.[59] The yield function and averaged transition probability are defined by

$$Y(\Gamma \to \Gamma') = Tr\{\rho(\Gamma) S \rho(\Gamma') S^{\dagger}\} \tag{B.3}$$

and

$$\omega(\Gamma \to \Gamma') = Y(\Gamma \to \Gamma') / Tr\{\rho(\Gamma)\} Tr\{\rho(\Gamma')\}. \tag{B.4}$$

The yield function $Y(\Gamma \to \Gamma')$ represents the sum of the transition probabilities while the probability function $\omega(\Gamma \to \Gamma')$ is the averaged transition probability, evaluated at a specified total energy E.

If $\rho(\Gamma)$ and $\rho(\Gamma')$ are separately invariant under time reversal, (not necessarily always the case) then both $Y(\Gamma \to \Gamma')$ and $\omega(\Gamma \to \Gamma')$ are also invariant, i.e.,

$$Y(\Gamma \to \Gamma') = Y(\Gamma' \to \Gamma) \equiv Y(\Gamma, \Gamma') \tag{B.5}$$

and similarly for $\omega(\Gamma, \Gamma')$. When $\rho(\Gamma)$ is a microcanonical distribution one can use the shorthand notation $Y(E)$ (or $\omega(E)$).

In general, it has been shown (i.e., Ref. 59, p. 143) that the time-reversed form of an operator, here denoted by a bar, is given by

$$\bar{\rho}(\Gamma) = \Theta \rho^{\dagger}(\Gamma) \Theta^{-1} \tag{B.6}$$

where Θ is the time-reversal operator. Since the density operator is Hermitian, it is time reversal invariant if

$$\bar{\rho}(\Gamma) = \Theta \rho(\Gamma) \Theta^{-1} = \rho(\Gamma). \tag{B.7}$$

Using the properties of the trace one can go through the following sequence of operations and show that $Y(\Gamma \to \Gamma') = Y(\Gamma' \to \Gamma)$.

If $\rho = \bar{\rho}$,

$$Tr\{\rho(\Gamma) S \rho(\Gamma') S^{\dagger}\} = Tr\{\rho(\Gamma') S^{\dagger} \rho(\Gamma) S\} \tag{B.8}$$

$$= Tr\{\Theta \rho(\Gamma') \Theta^{-1} S^{\dagger} \Theta \rho(\Gamma) \Theta^{-1} S\} = Tr\{\rho(\Gamma') \Theta^{-1} S^{\dagger} \Theta \rho(\Gamma) \Theta^{-1} S \Theta\}$$

From Eq. (B.6) (or Ref. 59, p. 147),

$$S = \Theta S^{\dagger} \Theta^{-1} \tag{B.9}$$

and since $\Theta^2 = \pm 1$,

$$S = \Theta^{-1} S^{\dagger} \Theta. \tag{B.10}$$

Thus the last term on the right hand side of Eq. (B.8) becomes

$$Tr[\rho(\Gamma') S \rho(\Gamma) S^{\dagger}],$$

seen to be the same as the first term (the l.h.s.) with Γ and Γ' interchanged.

Then

$$Y(\Gamma \to \Gamma') = Tr\{\rho(\Gamma) S \rho(\Gamma') S^{\dagger}\}$$

$$= Tr\{\rho(\Gamma') S \rho(\Gamma) S^{\dagger}\} = Y(\Gamma' \to \Gamma) \tag{B.11}$$

as expected, so

$$Y(\Gamma \to \Gamma') = Y(\Gamma' \to \Gamma) = Y(\Gamma, \Gamma') = Y(\Gamma', \Gamma). \tag{B.5}$$

Footnotes and References

1. For a review of recent developments in chemiluminescence, see T. Carrington and J. C. Polanyi, chapter in International Review of Science: Reaction Kinetics, MTP, Oxford (1972).
2. The first such study was that of (a) J. K. Cashion and J.C. Polanyi, J. Chem. Phys. 29, 455 (1958). See also (b) J. C. Polanyi, J. Chem. Phys. 34, 347 (1961).
3. An example of an extensive study is that of K.G. Anlauf,P.J. Kuntz, D. H. Maylotte, P.D. Pacey and J. C. Polanyi, Disc. Far. Soc. 44, 183 (1967).
4. See also (a) H. W. Chang, D. W. Setser, M. J. Perona and R.L.Johnson, Chem Phys. Letters 9 587 (1971); (b) H. W. Chang, D.W. Setser and M.J. Perona, J. Am. Chem. Soc. 75, 2070 (1971).
5. See also N. Jonathan, C. M. Melliar-Smith and D.H. Slater, Mol.Phys. 20, 93 (1971).
6. A summary of these "derived" translational distributions is given by K. G. Anlauf, P.E. Charters, D. S. Horne, R.G. Macdonald, D. H. Maylotte, J. C. Polanyi, W. J. Skrlac, D. C. Tardy and K. B. Woodall, J. Chem. Phys. 53, 4091 (1970).
7. The first such study was that of (a) A.E. Grosser, A.R. Blythe and R.B. Bernstein,J. Chem. Phys. 42, 1268 (1965).A more recent one is (b) K.T. Gillen, A.M. Rulis and R.B. Bernstein, J. Chem. Phys. 54, 2831 (1971).
8. An early study is that of (a) J.H. Birely and D.R. Herschbach, J. Chem. Phys. 44, 1690 (1966). A more recent one is (b) J.D. McDonald, P.R. LeBreton, Y.T. Lee and D.R. Herschbach, J. Chem. Phys. 56, 769 (1972).
9. See also J. B. Cross and N.C. Blais, J. Chem. Phys. 55, 3970(1971); ibid., 52, 3580 (1970).
10. For a review of experimental developments in reactive scattering, see J.L. Kinsey, chapter in International Review of Science:Reaction Kinetics, MTP, Oxford (1972).

11. The first such study was that of (a) R.R. Herm and D.R. Herschbach, J. Chem. Phys. 43, 2139 (1965). See also (b) C.Maltz and D.R. Herschbach, Disc. Far. Soc. 44, 176 (1967).
12. A recent one is that of R. Grice, J.E. Mosch, S.A. Safron and J.P. Toennies, J.Chem. Phys. 53, 3376 (1970).
13. The first such study was that of S.M. Freund, G.A. Fisk, D.R. Herschbach and W. Klemperer, J. Chem. Phys. 54, 2510 (1971).
14. A recent one is that of H.G. Bennewitz, R. Haerten, and G. Müller, Chem. Phys. Letters 12, 335 (1971).
15. See, for example, (a) M.J. Berry and G.C. Pimentel, J. Chem. Phys. 49, 5190 (1968). Also, (b) J.H. Parker and G.C. Pimentel, J. Chem. Phys. 51, 91 (1969); ibid., 55, 857 (1971).
16. See also M.C. Lin and W.H. Green, J. Chem. Phys. 53, 3383 (1970).
17. The first such study was that of A.L. Schmeltekopf, E.E. Ferguson and F.C.Fehsenfeld, J. Chem. Phys. 48, 2966 (1966). See also, for example, D.H. Stedman, D. Steffenson and H. Niki, Chem. Phys. Letters 7, 173 (1970).
18. (a) W.A. Chupka and M.E. Russell, J. Chem. Phys. 49, 5426 (1968), (b) W.A. Chupka, J. Berkowitz and M.E. Russell, Abstracts VI ICPEAC, M.I.T., Cambridge, Mass. (1969), p. 71.
19. T.J. Odiorne, P.R. Brooks and J.V. Kasper, J. Chem. Phys. 55, 1980 (1971).
20. M.J. Berry and G.C. Pimentel, J. Chem. Phys. 51, 2274 (1970); ibid., 53, 3453 (1971).
21. For a review, see C.B. Moore, Ann. Rev. Phys. Chem. 22, 387 (1971).
22. See, for example, R.B. Bernstein, Israel J. Chem. 9, 0000 (1971) and refs. therein.
23. For a review of theoretical-computational developments in reactive scattering, see R.D. Levine, chapter in International Review of Science: Theoretical Chemistry, MTP, Oxford (1972).
24. K.G. Anlauf, D.H. Maylotte, J.C.Polanyi and R.B. Bernstein, J. Chem. Phys. 51, 5716 (1969).
25. J.L.Kinsey, J. Chem. Phys. 54, 1206 (1971).
26. R.A. Marcus, J. Chem. Phys. 53, 604 (1970).

27. See, for example, (a) R.D. Levine, F.A. Wolf and J.A. Maus, Chem. Phys. Letters 10, 2 (1971), and (b) R.D. Levine and R.B. Bernstein, Chem. Phys. Letters 11, 552 (1971).
28. E.E. Nikitin, Theor. Exptl. Chem. 1, 83, 90 (1965).
29. J.C. Light, Disc. Far. Soc. 44, 14 (1967).
30. See also D.G. Truhlar, J. Chem. Phys. 54, 2635 (1971).
31. For a review of quantal treatment of reactive scattering, see J.C. Light, Adv. Chem. Phys. 19, 1 (1971).
32. For a review of classical trajectory methods, see D.L. Bunker, Method. Comput. Phys. 10, 287 (1971).
33. See, for example, (a) L.M. Raff, L.B. Sims, D.L. Thompson and R.N. Porter, J. Chem. Phys. 53, 1606 (1970); B.H. Mok and J.C. Polanyi, J. Chem. Phys. 53, 4588 (1970) and refs. therein.
34. See also J.T. Muckerman, J. Chem. Phys. 54, 1164 (1971); ibid., 56, 0000 (1972).
35. For a review, see P.J. Kuntz, Electronic and Atomic Collisions, Invited Papers, VII ICPEAC, North-Holland Press, Amsterdam (1971).
36. M. Karplus, chapter in C. Schlier, Ed., Molecular Beams and Reaction Kinetics, Academic Press, N.Y. (1970), p. 372, and refs. therein.
37. For a review of reactive scattering of ions and molecules, see E.W. McDaniel, V. Cermak, A. Dalgarno, E.E. Ferguson and L. Friedman, Ion-Molecule Reactions, Wiley-Interscience, N.Y. (1970).
38. The first such study was that of A.P.M. Baede, A.M.C. Moutinho, A.E. deVries and J. Los, Chem. Phys. Letters 3, 530 (1969). See also (b) A.M.C. Moutinho, J.A. Aten and J. Los, Abstracts VII ICPEAC, North-Holland Press, Amsterdam (1971) p. 280.
39. Another early study was that of R.K.B. Helbing and E.W. Rothe, J. Chem. Phys. 51, 1607 (1969).
40. See also R.M. Compton, S.J. Nalley, H.C. Schweinler and V.E. Anderson, Abstracts VII ICPEAC, North-Holland Press, Amsterdam (1971), p.288.
41. M.E. Gersh and R.B. Bernstein, J. Chem. Phys. 55, 4661 (1971).
42. F.P. Tully, Y.T. Lee and R.S. Berry, Chem. Phys. Letters 9, 80 (1971).

43. C.F. Giese, Chap. 2 in P.J. Ausloos, Ed., Ion Molecule Reactions in the Gas Phase, ACS Advances in Chemistry Series No. 58 (1966), p. 20.

44. (a) C.A. Coulson and R.D. Levine, J. Chem. Phys. 47, 1235 (1967); (b) R.D. Levine, Quantum Mechanics of Molecular Rate Processes, Clarendon Press (Oxford 1969), Sec. 2.8.2 .

45. For a variety of reactions which show either "spectator-stripping" or "complex" formation behavior, $E_{T'}^{(m)}$, is found to be proportional to E_T[46]. Thus, for $E_T >> -\Delta E_o$, $f_{T'}^{(m)}$ is nearly independent of E. Of course, $f_{R'}^{(m)}$, or $f_{V'}^{(m)}$ may vary with E, but will probably vary less strongly than will $E_{R'}^{(m)}$ or $E_{V'}^{(m)}$.

46. A. Henglein, chapter in C. Schlier, Ed., Molecular Beams and Reaction Kinetics, Academic Press, N.Y. (1970), p. 139.

47. The triangular contour maps of Anlauf et al.[24], Polanyi and Tardy[48] and Kinsey[25], constructed for the inverse (endoergic) reaction from data obtained on the reaction studied in the forward (exoergic) direction, are of this type.

48. J.C. Polanyi and D.C. Tardy, J. Chem. Phys. 51, 5717 (1969).

49. For examples of such calculations dealing with the role of vibrational excitation of reactants see (a) J.B. Anderson, J. Chem. Phys. 52, 3849 (1970) and (b) R.L. Jaffe and J.B. Anderson, J. Chem. Phys. 54, 2224 (1971).

50. Structural features of the $\underset{\sim}{P}$-matrix for inelastic scattering (rotational excitation of a diatomic rigid rotor) have been pointed out by (a) W.A. Lester, Jr. and R.B. Bernstein, Chem. Phys. Letters 1, 207, 347 (1967), (b) R.D. Levine and B.R. Johnson, Chem. Phys. Letters 4, 365 (1969) and (c) W.A. Lester, Jr. and R.B. Bernstein, J. Chem. Phys. 53, 11 (1970). A "matrix shape" approach to inelastic scattering has been proposed by (d) H.A. Rabitz, J.Chem.Phys. 55, 407 (1971).

51. R.A. LaBudde, private communication (1971). p.d.f. denotes probability density function.

52. The original work is that of (a) C.E. Shannon, Bell System Tech. J. 27, 379, 623 (1948); it is reprinted in (b) C.E. Shannon and W. Weaver, The Mathematical Theory of Communication, University of Illinois Press, Urbana (1949).

53. E.T. Jaynes, Phys. Rev. 106, 620 (1957); ibid., 108, 171 (1957).

54. A.I. Khinchin, Mathematical Foundations of Information Theory, Dover, New York (1957).

55. A. Katz, Principles of Statistical Mechanics, Freeman, San Francisco (1967).

56. J.E. Mayer and M.G. Mayer, Statistical Mechanics, J. Wiley, N.Y. (1940), p. 436.

57. One cannot in practice specify the initial orbital angular momentum. Equally, in the absence of a field, one cannot specify orientation quantum numbers, etc. Thus, all these different states are usually counted together. Similarly, when the initial group γ is the group of all initial orientation quantum numbers, all final orientation quantum numbers (in the absence of a field) are indistinguishable and have to be counted together as a group γ'.

58. J. Ross, J.C. Light and K.E. Shuler, chapter in Kinetic Processes in Gases and Plasmas, Academic Press, N.Y. (1969), p. 281.

59. R.D. Levine, Quantum Mechanics of Molecular Rate Processes, Clarendon Press, Oxford (1969).

60. C.A. Coulson and R.D. Levine, J. Chem. Phys. 47, 1235 (1967).

61. R.C. Tolman, Statistical Mechanics, Clarendon Press, Oxford (1938).

62. M. Tribus, Thermostatics and Thermodynamics, Van Nostrand, N.Y. (1961), p. 64.

63. From Ref. 54, p. 4, it is seen that the average of a convex function is larger than the value of the function at the average argument. In the present notation, if $f''(x) > 0$, $\sum_\Gamma P_\Gamma f(x_\Gamma) \geq f(\sum_\Gamma P_\Gamma x_\Gamma)$.

64. L.T. Cowley, D.S. Horne and J.C. Polanyi, Chem. Phys. Letters 12, 144 (1971).

65. C. Kittel, Elementary Statistical Physics, J. Wiley, N.Y. (1958), p. 172.

66. L. Brillouin, Science and Information Theory, Academic Press, New York (1956).

67. The $\Delta S'$ obtained from "poor man's" inclusive data (where $I_p = -\lg\omega(\Gamma,\Gamma')$) would be positive, but may be much smaller than that obtained from averaging over specific inclusive data (where we obtain $I_p = -\sum_{\gamma'} P_{\gamma'} \lg\omega(\Gamma,\gamma')$). The upper bound for $\Delta S'$ is provided by the I_p obtained as an average over specific clusive data. (This intrinsic value is $I_p = -\sum_{\gamma'} P_{\gamma'} \sum_{\gamma} P_{\gamma} \lg\omega(\gamma,\gamma')$). These considerations, which follow as in (44), imply that every constraint imposed on the possible freedom of choice of the initial state immediately results in the <u>decrease</u> of $\Delta S'$. An extensive discussion of the three information measures mentioned above will be given in a later paper in this series.

68. Of course, there can be an infinite variety of product distributions (or $\underline{P}$-matrices) with the same $\Delta S'$, so it alone is by no means a unique characterization of the distribution. As is well known, one requires all the moments of a probability density function to characterize it uniquely. However, $\Delta S'$ and the two independent first moments (<u>e.g.</u>, $\langle \Delta E'_{tr} \rangle$ and $\langle \Delta E'_{vib} \rangle$, etc.) together serve to specify most of the physically interesting features of the reactive scattering behavior for the microcanonical ensemble at the specified E. This has the macroscopic analogy: for a canonical system at a temperature T, we may "characterize" the reaction by ΔS^o and ΔE^o (or ΔH^o).

Legend for Figures

1. (a) Contour map of $\omega(E_T, E_{T'})$ at a fixed value of the total energy, $E = 10$ units, for a (hypothetical) exoergic reaction for which $-\Delta E_o = 5$ units. Thus E_T and $E_{T'}$ range from 0 to 5 and 0 to 10 units, respectively. (b) A square-faced bar plot $\omega(f_T, f_{T'})$ for the same reaction, showing the dependence of the contour map upon the total energy, over the range $10 \leq E \leq 50$ units. The "trajectory" of the maximum of ω as a function of E appears as the heavy curve passing down the length of the bar. For the purpose of drawing the results in (a) and (b) they were scaled such that, at the maximum, ω has been assigned the value 1, i.e., $\omega^{(m)}(E) = 1$. (A similar comment applies to Figs. 3-5.) An actual experiment (or computation) would also provide the energy dependence of the peak value, $\omega^{(m)}(E)$. Thus, besides Fig. 1(c) one would also require a figure showing $\omega^{(m)}$ vs. E. (c) The coordinates of the loci of the maximum, i.e., $f_T^{(m)}$ and $f_{T'}^{(m)}$, plotted vs. total energy E over the same range as in (b).

2. Comparison of the effect of E_V with that of E_T upon the total reaction cross section for the reaction $N_2(v) + O^+ \rightarrow NO^+ + N$ ($\Delta E_o = 1.1$eV). The E_V dependence is taken from Ref. 17, while the E_T dependence is from Ref. 43.

3. Triangular product contour map of $\omega(f_{T'}, f_{V'}, f_{R'}; f_V, f_R)$ for some fixed (but here unspecified) f_V, f_R, E. In the example shown, the locus of the most probable ω is $f_{T'} = 0.15$, $f_{R'} = 0.25$, $f_{V'} = 0.60$ (most of the available energy going into product vibrational excitation). Here and in Fig. 4 the triangular maps represent the results of specific clusive experiments. (cf. Sec. 8).

4. (a) Prismatic plot of $\omega(f_{T'}, f_{V'}, f_{R'}, f_V, f_R)$ showing the dependence of the triangular contour map of Fig. 2 upon the total energy E ($5 \leq E \leq 20$ units). (b) The coordinates of the loci of the maximum, i.e. $f_{T'}^{(m)}$, $f_{V'}^{(m)}$, $f_{R'}^{(m)}$, plotted vs. E over the same range as in (a).

5. "Decomposition" of a single point on the square contour map $\omega(f_T, f_{T'})$ into its two "components", i.e., cuts through the two triangular contour maps $\omega(f_V, f_R, a; f_{T'})$ and $\omega(f_{V'}, f_{R'}, b; f_T)$. The global maps here and in Fig. 1 are global inclusive representations. Thus these triangular maps represent specific inclusive experiments.

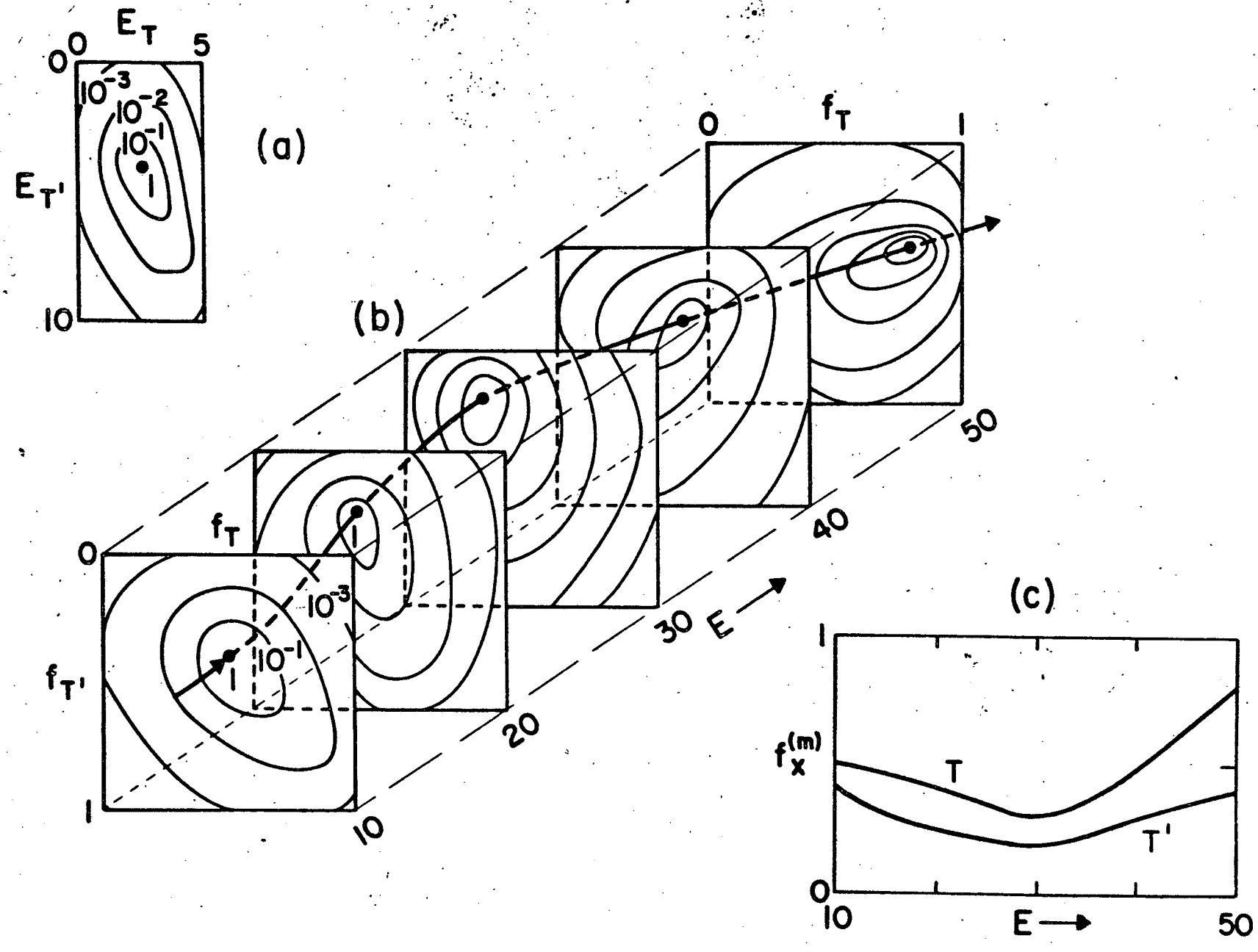

FIGURE 1

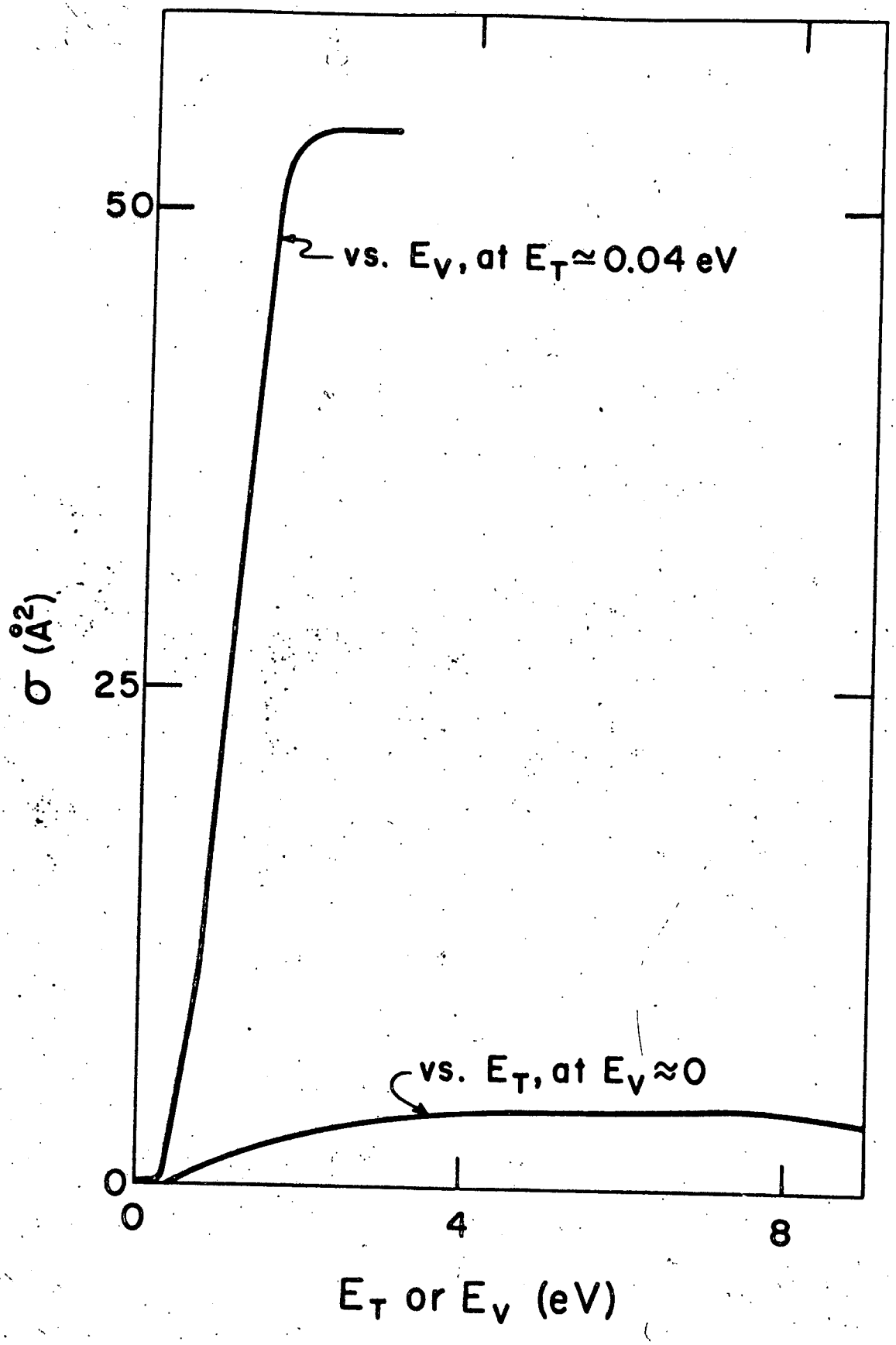
50
25
0
0
4
8
σ (Å²)
vs. E_V, at $E_T \simeq 0.04$ eV
vs. E_T, at $E_V \approx 0$
E_T or E_V (eV)

FIGURE 2

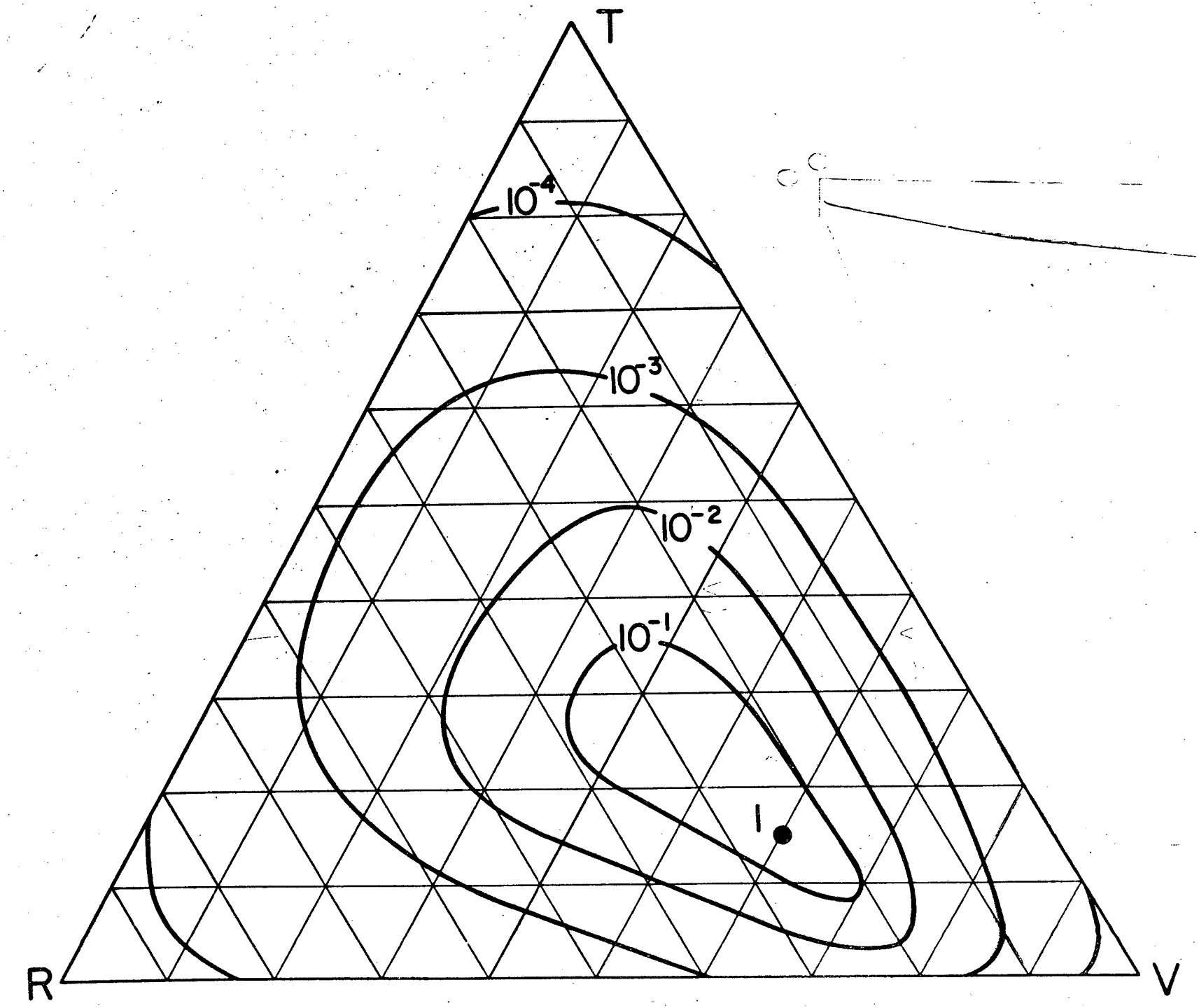

FIGURE 3

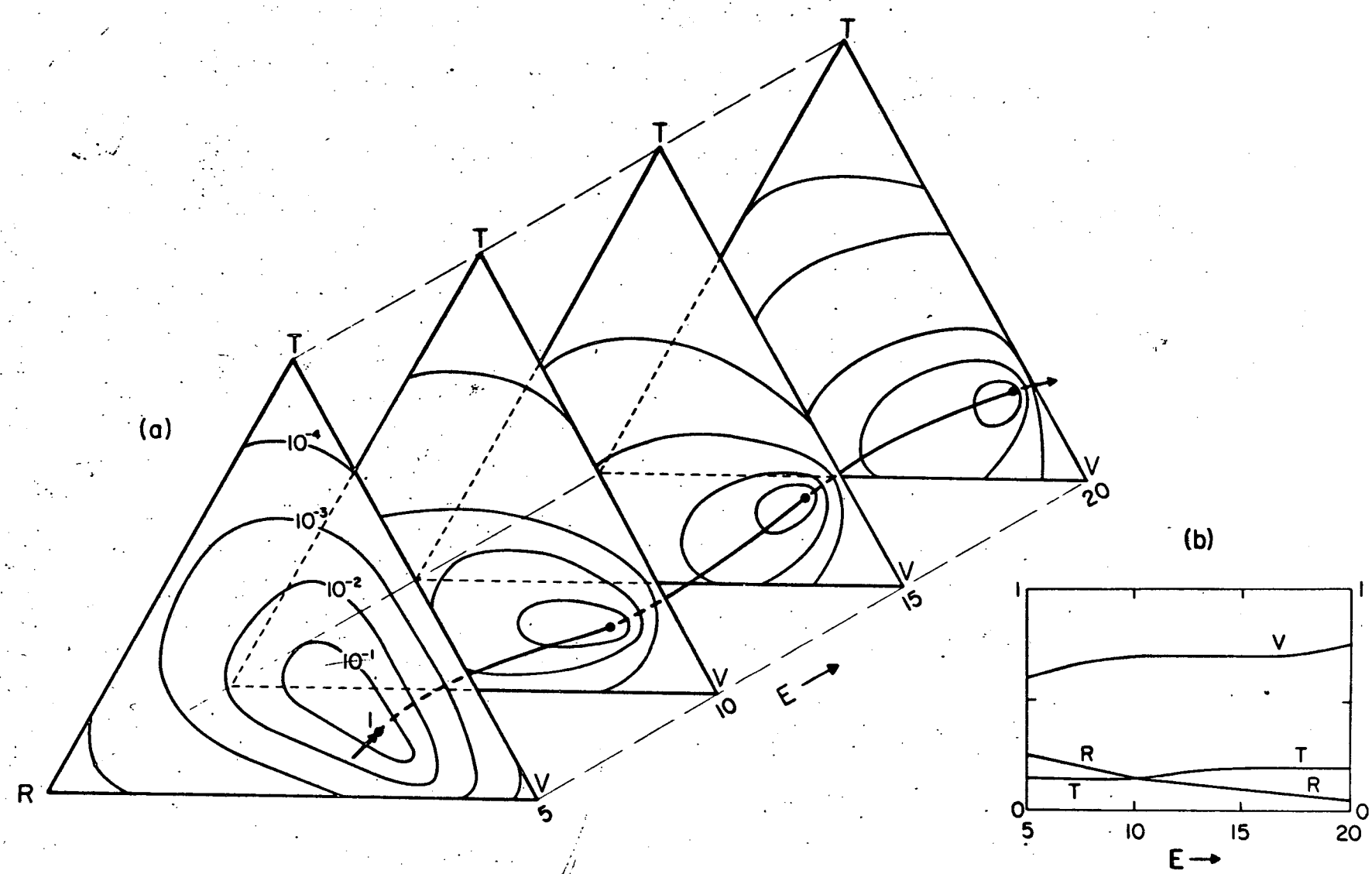

FIGURE 4

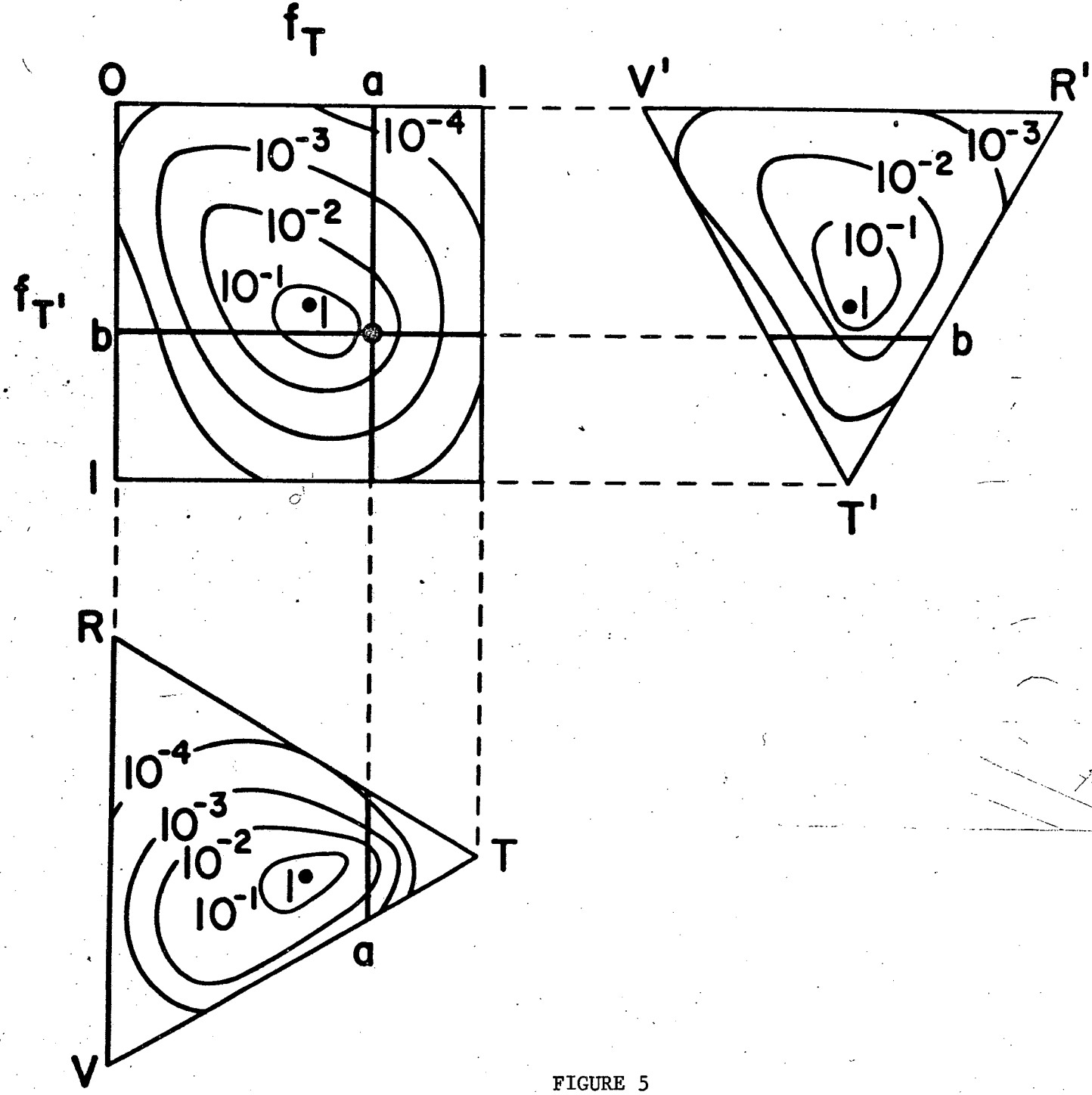

FIGURE 5